Nanoscale Advances

ROYAL SOCIETY OF CHEMISTRY

PAPER

View Article Online
View Journal | View Issue

Open Access Article. Published on 25 April 2023. Downloaded on 1/10/2026 11:10:29 PM.
This article is licensed under a Creative Commons Attribution-NonCommercial 3.0 Unported Licence.

Check for updates

Cite this: *Nanoscale Adv.*, 2023, **5**, 2950

Titanate nanotubes as an efficient oral detoxifying agent against drug overdose: application in rat acetaminophen poisoning†

Abir Salek,‡[a] Mouna Selmi,‡[a] Leila Njim,[b] Polona Umek,[c] Philippe Mejanelle,[d] Fathi Moussa,[e] Wahiba Douki,[f] Karim Hosni[a] and Tarek Baati *[a]

Voluntary drug intoxication is mainly due to drug overdose or the interaction of several drugs. Coma and its associated complications such as hypoventilation, aspiration pneumopathy, and heart rhythm disorders are the main hallmarks of drug intoxication. Conventional detoxification treatments, including gastric lavage or vomiting, administration of ipecac or activated charcoal (CH), and the use of antidotes, have proven to be inefficient and are generally associated with severe adverse effects. To overcome these limitations, titanate nanotubes (TiNTs) are proposed as an efficient emerging detoxifying agent because of their tubular shape and high adsorption capacity. In the present study, the detoxifying ability of TiNTs was evaluated on paracetamol (PR)-intoxicated rats. Results indicate that the loading ability of PR into TiNTs (70%) was significantly higher than that recorded for CH (38.6%). In simulated intestinal medium, TiNTs showed a controlled drug release of less than 10% after 72 h of incubation. In PR-intoxicated rats, TiNTs treatment resulted in a 64% decrease of PR after 4 h of poisoning *versus* 40% for CH. Concomitantly, TiNTs efficiently reduced PR absorption by 90% after 24 h of poisoning, attenuated the elevated levels of biochemical markers (*i.e.*, alanine aminotransferase, aspartate aminotransferase, creatinine, and TNF-α) and mitigated oxidative stress by increasing the activity of superoxide dismutase and reducing the oxidized glutathione/total glutathione ratio, suggesting a histoprotective effect of TiNTs against paracetamol-induced toxicity in rats. In addition to their safety and high stability in the entire gastro-intestinal tract, biodistribution analysis revealed that TiNTs exhibited low intestinal absorption owing to their large cluster size of compact aggregate nanomaterials across the intestinal villi hindering the absorption of paracetamol. Collectively, these data provide a new and promising solution for *in vivo* detoxification. TiNTs are expected to have great potential for the treatment of voluntary and accidental intoxication in emergency care.

Received 30th November 2022
Accepted 22nd April 2023

DOI: 10.1039/d2na00874b

rsc.li/nanoscale-advances

1. Introduction

Voluntary drug intoxication is found in suicide attempts, which are a social problem particularly in adolescents,[1] drug addiction or criminal poisonings.[2] According to the Health Watch Institute, voluntary drug intoxication caused the death of more than 70 000 people in the USA and 5000 people in Europe in 2017.[3,4] In England and Wales, 4859 deaths related to drug poisoning were recorded in 2021 according to the National Statistics Office, which presents a rate of 84.4 deaths per million inhabitants; this is 6.2% higher than the rate recorded in 2020 (79.5 deaths per million).[5] In the United States, the rate of drug overdose deaths increased by 14% from 2020 to 2021, from 28.3 to 32.4. Indeed, among the total population, 106 699 drug overdose deaths occurred, resulting in an age-adjusted rate of 32.4 per 100 000 standard population.[6] In France, suicide attempts amount to more than 200 000 per year; more than three quarters of cases are voluntary drug poisoning by ingestion of psychotropic drugs.[7] The high frequency of overdosed patients admitted in the casualty department and the high healthcare consumption associated with this pathology make it a major public health issue.[8] Indeed, the main complications of drug intoxication are essentially coma and its resulting

[a]Laboratoire des Substances Naturelles, Institut National de Recherche et d'Analyse Physico-chimique, Biotechpôle Sidi Thabet, 2020, Tunisia. E-mail: tarek.baati@gmail.com; Fax: +216 71 537 688; Tel: +216 71 537 666

[b]Service d'Anatomie Pathologique, EPS Fattouma Bourguiba de Monastir, Faculté de Médecine de Monastir, Université de Monastir, 5000 Monastir, Tunisia

[c]Jožef Stefan Institute, Jamova cesta 39, SI-1000 Ljubljana, Slovenia

[d]Département de chimie, IUT d'Orsay, Université Paris-Saclay, 91190 Gif-sur-Yvette, France

[e]Institut de Chimie Physique, CNRS UMR 8000, Université Paris-Saclay, 91190 Gif-sur-Yvette, France

[f]Laboratoire de Biochimie et de Toxicologie, EPS Fattouma Bourguiba de Monastir, Université de Monastir, 5000 Monastir, Tunisia

† Electronic supplementary information (ESI) available. See DOI: https://doi.org/10.1039/d2na00874b

‡ Abir Salek and Mouna Selmi contributed equally.

© 2023 The Author(s). Published by the Royal Society of Chemistry

Open Access Article. Published on 25 April 2023. Downloaded on 1/10/2026 11:10:29 PM.
This article is licensed under a Creative Commons Attribution-NonCommercial 3.0 Unported Licence.

hypoventilation, aspiration pneumopathy and heart rhythm disorders, which lead to increases in intensive care admissions, length of hospital stay and mortality.[9] Unfortunately, the use of pharmacological antidotes is limited because of their unavailability for all drugs or toxins, notably when the poisoning substance is unknown.[10] Except for activated charcoal (CH), detoxification procedures and the use of antidotes can result in severe adverse effects.[11] Regarding CH, despite its rapid (2 to 3 hours after intoxication) and good detoxifying ability for many xenobiotics,[12,13] several drugs still present poor affinity for this material, thus reducing its efficacy even with repeated administration.[12,14] Hence, the search for novel strategies that provide alternative approaches to these detoxifying methods is a challenging task. Porous biocompatible nanomaterials with high stability in the gastrointestinal environment could provide an approach for better detoxification efficiency while reducing the adverse effects of conventional methods. In this regard, we recently developed micrometric Fe-based porous MOFs materials (MIL-127) and successfully applied them for the detoxification of salicylate poisoned rats.[15] In addition, a Ti-based porous MOF material (MIL-125-NH_2) was tested for the detoxification of salicylate and was able to reduce twofold the salicylate concentration peak in blood compared with activated charcoal.[16] Although there has been success with MOF materials, there are some limitations regarding their application because of their average reduction of drug overdose (only twofold compared to that of activated charcoal), high cost, laborious synthesis, low yield and the paucity of information regarding the main parameters influencing the oral detoxification process, including particle size, absorption and biodistribution *in vivo* experiments.[15] To overcome these limitations, the use of other cheap and efficient biocompatible nanomaterials could represent a good option. Titanium nanotubes (TiNTs) are proposed as a highly promising alternative because of their simple and rapid synthesis process, as well as their high yield (10 g by chemical reaction). These porous materials with multilayered elongated tubes have a tunable shape open at both ends with a length mean ranging from 80 nm to 1 μm, a significant pore volume around 0.67 $cm^3\ g^{-1}$ characterized by a high surface area ($S_{BET} = 270\ m^2\ g^{-1}$), and a size of 10 nm in the outer diameter and 4 nm in the inner diameter,[17,18] making them advantageous over cubic MOF micro-particles. The tunable shape of TiNTs improves their deep internalization between cell membranes even if they aggregate[17,18] and consequently increases their contact with the drug and its entrapment inside. These unique geometrical properties play an important role not only in increasing drug entrapment and loading inside TiNTs but also in the drug delivery process and its sustained release.[17–21] Compared to carbon nanotubes or to spherical and hybrid nanomaterials, TiNTs exhibited a higher capacity for drug loading and perfect biocompatibility.[22–27] Indeed, the toxicity of these materials, their pharmacokinetic profile, and their biodistribution were studied at 45 days following an intravenous injection of 45 mg kg^{-1} in mice. The histological examination of organs and the analysis of liver and kidney function markers and the inflammatory response confirmed the long-term innocuity of these nanomaterials. The parameters of pharmacokinetics revealed the rapid clearing of TiNTs from the bloodstream by 6 h after intravenous injection; the main accumulation was in the liver and spleen and their degradation and clearance from these tissues were relatively slow (>4 weeks). Interestingly, an important property of these materials is their slow dissolution under a lysosome acid environment, rendering them biodegradable. It is noteworthy that TiNTs were directly eliminated in urine and bile ducts without obvious toxicity in mice. Moreover, these nanomaterials are highly stable in most biological media at neutral pH, as we have proved in the simulated intestinal medium and cell culture medium.[17] Regarding these physicochemical properties and safety, TiNTs could be considered a perfect substitute for CH in the anti-poisoning process. From this perspective, we propose in this work to study the efficiency of TiNTs as an oral detoxifying agent against poisoning, with paracetamol (PR) used as a drug model. PR is frequently involved in many voluntary or accidental intoxications[28] since it is the most common analgesic treatment available without a medical prescription. Currently, the medical literature on paracetamol is oriented towards the toxicological and pharmacological side, in search of factors causing the hepatotoxicity of this analgesic long considered for its safety of use, and in the elucidation of its mechanisms of analgesic action. A retrospective study places PR in 3rd position, at 11.7%, of drugs found in voluntary poisonings, behind benzodiazepines (76.9%) and neuroleptics (18.4%).[29] The toxicity of PR is of the lesion type and it is irreversible because its metabolization creates *N*-acetyl-*p*-benzoquinone imine (NAPQI), a compound highly toxic for the liver.[30,31] Herein, we first studied the *in vitro* stability of TiNTs in simulated gastrointestinal (GI) conditions, then determined the PR/TiNTs loading capacity as well as the kinetics of its release. Secondly, the efficiency of TiNTs in PR detoxification was monitored at different times by chromatographic analysis of the drug serum collected from the overdosed-rats co-treated with TiNTs and compared to those of the overdosed-rats co-treated with CH. The percentage of PR absorbed in the presence of TiNTs or CH after the rats' poisoning was determined. Finally, the toxicity of TiNTs, their distribution profile and elimination were studied through the assessment of biochemical parameters and histopathological examination of the untreated control and TiNTs- and CH-treated animals.

2. Materials and methods

2.1 TiNTs synthesis and characterization

TiNTs were prepared by a classical hydrothermal method and characterized as described previously.[22] TiNTs powder was appropriately suspended in pure water (0.1 mg mL^{-1}), then ultrasonicated for 5 min. A sample of 20 μL was observed using a transmission electron microscope (TEM, Tecnai G2, FEI, Netherlands) at 200 kV and images were acquired with a Veleta camera (Olympus, Japan). TiNTs powder was also characterized by SEM using a ZEISS Sigma scanning electron microscope (SEM) with a 10 kV accelerating voltage. For crystallinity, X-ray diffraction (XRD) was performed at room temperature with an

Open Access Article. Published on 25 April 2023. Downloaded on 1/10/2026 11:10:29 PM.
This article is licensed under a Creative Commons Attribution-NonCommercial 3.0 Unported Licence.

X-ray diffractometer (X′ Pert PRO MPD, PANalytical Co., Holland). Monochromatic Cu Kα-radiation ($\lambda = 1.5418$ Å) was obtained with Ni-filtration and a system of diverging and receiving slides of 0.5° and 0.1 mm, respectively. The diffraction pattern was measured at a voltage of 40 kV and a current of 30 mA over a 2θ range of 3–40° using a step size of 0.02° at a scan speed of 1 s per step.

2.2 TiNTs stability study

TiNTs stability was studied in HCl solution and Ringer's medium as simulated gastric and intestinal conditions, respectively. Gastrointestinal conditions (GI) were reproduced as in healthy vertebrates.[32] The study was performed by suspending 1 mg of TiNTs in 100 mL of an HCl solution at pH = 1.2 (0.137 M) or in 100 mL of Ringer's solution at pH = 6.2. All suspensions were stirred under bidimensional continuous stirring in an incubator at 60 × 60 rpm at 37 °C for 24 h. Then, all samples were centrifuged at 14 500 rpm for 10 minutes in order to recover the solid and liquid phases. To check the stability of TiNTs, the crystallinity and porosity of the recovered powder were investigated by XRD and N_2 isotherm analysis, respectively, and compared to those of the pristine TiNTs. Moreover, the percentage of Ti released in the supernatant was determined by ICP-OES on a PerkinElmer Optima 7300 DV, as reported previously.[22]

2.3 Paracetamol/TiNTs loading

A fixed concentration of PR (2 mg mL^{-1}) was prepared in Ringer's solution at pH = 7.2. This concentration corresponds to that administered in the rats to induce poisoning. For entrapment tests, TiNTs powder was dehydrated at 70 °C for 16 hours to remove water and residual solvent from the pores. Different PR : TiNTs mass ratios were tested for drug loading capacity, including 1 : 0.5, 1 : 1, 1 : 2, 1 : 4 and 1 : 5. Drug loading was performed by suspending the equivalent mass ratio of TiNTs powder in 5 mL of PR solution under continuous magnetic stirring for 24 h at 37 °C. For each entrapment time (3, 6 and 24 h), the samples were prepared in triplicate. The efficient TiNTs mass ratios leading to the optimal drug loading capacity were compared to the same mass ratio of Norit® activated charcoal (CH) in the same conditions. To determine the concentration of unabsorbed paracetamol, samples were centrifuged for 15 min at 14 000 rpm to recover the supernatant prior to analysis by high-performance liquid chromatography (see Section 2.8). Likewise, the level of PR entrapped inside the TiNTs was determined by thermogravimetric analysis (TGA). The percentage of drug loading was determined according to the following formula: (initial quantity − final quantity)/initial quantity × 100. Finally, more characterization through XRD patterns, FTIR spectra and N_2 isotherms was performed on TiNTs 24 h after the PR loading and the results were compared to those of the empty nanotubes.

2.4 *In vitro* drug release

PR release was carried out in triplicate by soaking 5 mg of PR-loaded-TiNTs in 20 mL of Ringer's solution (0.04 M, pH 7.2) at 37 °C under continuous bidimensional stirring (120 rpm, Multitron Ortibale incubator, 50 mm, HT Infors, France). In order to determine the kinetics of PR release, 10 samples of 1 mL were recovered from the supernatant obtained after centrifugation at 14 500 rpm for 15 min, from 5 min post stirring up to 72 h. Samples were recovered and replaced with the same volume of fresh medium at 37 °C. The drug concentration in the supernatants was then determined by HPLC (see Section 2.8).

2.5 Thermogravimetric analysis (TGA)

For TGA measurements, TiNTs or PR/TiNTs samples (5 mg) were analyzed under oxygen flow (20 mL min^{-1}) using a PerkinElmer Diamond TGA/DTA STA 6000 from room temperature (25 °C) to 800 °C with a scan rate of 10 °C min^{-1}. The amount of PR was estimated by considering the weight loss of the empty and dried TiNTs (mg of PR per 100 mg of dry TiNTs).

2.6 FTIR spectra and N_2 isotherms

Fourier transform infrared spectroscopy (FTIR) studies were recorded on TiNTs powder using a Nicolet 6700 FTIR Thermo Scientific spectrometer in the 500–4000 cm^{-1} region.

For the N_2 sorption experiments, a degassing step was first applied to clean the samples by removing everything adsorbed on their surface. Approximately 40 mg of materials was evacuated following a two-step process: a high vacuum (10^{-6} mmHg) at 80 °C for 12 h and then under secondary vacuum directly in the Belsorp Max instrument at 100 °C for 5 h. N_2 isotherms were obtained at 77 K using a Belsorp Max (Bel Japan). Prior to the analysis, the samples' BET surface area and nanopore volume were estimated at a relative pressure lower than 0.25.

2.7 *In vivo* experiments

Gastrointestinal decontamination of drug overdose was performed in rats using the optimum mass ratio of PR : TiNTs obtained *in vitro* (*i.e.*, 1 : 5), corresponding to 10 g kg^{-1} of TiNTs and 2000 mg kg^{-1} of paracetamol, which is ten times higher than the therapeutic dose prescribed for rat or mouse and is 80% of the median lethal dose (DL50 : 2500 mg kg^{-1}).[33] In addition, the safety and biodistribution of TiNTs were addressed for the first time after oral administration.

2.7.1 Animals. Animal care procedures were conducted in conformity with the legislation for the protection of animals used for scientific purposes provided by the relevant Tunisian law and European Union Directive (Tunisian Legislative Decree 2009-2200 and 2010/63/EU) and the International Guiding Principles for the Biomedical Research Involving Animals (Council for the International Organizations of Medical Sciences, CH). Animals were subjected to experimental protocols approved by the Animal Ethics Committee of the Faculty of Veterinary Medicine of Sidi Thabet (permit number CEBM 3.2021). All adequate measures were taken to minimize animal pain or discomfort and all surgery was performed under mild anesthesia. Thirty-six (36) Wistar male rats (5 weeks old, 50 ± 15 g) were obtained from the Tunisian Society of Pharmaceutical Industries and Laboratory (SIPHAT, Ben Arous, Tunisia). All

 © 2023 The Author(s). Published by the Royal Society of Chemistry

Open Access Article. Published on 25 April 2023. Downloaded on 1/10/2026 11:10:29 PM.
This article is licensed under a Creative Commons Attribution-NonCommercial 3.0 Unported Licence.

animals were maintained in an air-conditioned room (22–25 °C) on a 12 h light/dark cycle with water and food available. To evaluate the efficacy of TiNTs as a detoxifying agent, animals were fasted 24 h before experiments.

2.7.2 Experimental design. Animals were randomly divided into six groups of 6 animals each ($n = 6$) and all treatments were administered by oral gavage.

• Group 1 (control): rats receiving 1 mL of Ringer's solution.

• Group 2 (TiNTs-24 h): rats receiving 1 g kg^{-1} of TiNTs followed (after 1 h) by 1 mL of Ringer's solution to act for 24 h.

• Group 3 (CH-24 h): rats receiving 1 g kg^{-1} of Norit® activated charcoal followed (after 1 h) by 1 mL of Ringer's solution to act for 24 h.

• Group 4 (positive control PR-24 h): rats receiving 2000 mg kg^{-1} of PR which was first suspended in 1 mL of Ringer's solution then sonicated. After 1 h, 1 mL of Ringer's solution was orally administered to act for 24 h.

• Group 5 (PR-TiNTs-24 h): rats receiving 2000 mg kg^{-1} of PR which was first suspended in 1 mL of Ringer's solution then sonicated. After 1 h, 1 g kg^{-1} of TiNTs was dispersed and sonicated in Ringer's solution (1 mL) and then orally administered to act for 24 h.

• Group 6 (PR-CH-24): rats receiving 2000 mg kg^{-1} of PR which was first suspended in 1 mL of Ringer's solution then sonicated. After 1 h, 1 g kg^{-1} of CH was dispersed and sonicated in Ringer's solution (1 mL) and then orally administered to act for 24 h.

Four hours after the rats' treatment, 200 μL of blood was collected from the tail vein for serum PR concentration determination. The efficacy of TiNTs as a detoxifying agent was compared to that of activated charcoal, a currently available detoxification method.

All animals were placed in individual metabolic cages 24 h before sacrifice to collect urine and feces. Animals were then anesthetized under isoflurane and sacrificed. The blood samples were collected by intra-cardiac puncture, inoculated in heparin tubes, and centrifuged at 3600 rpm to separate serum. Serum samples were aliquoted then stored at −80 °C until analysis. Organs including liver, spleen, heart, lungs, kidneys and brain were extracted, washed with 0.9% NaCl at 4 °C and stored at −20 °C as reported previously.[28,34]

For histological evaluation, organs were excised, fixed in 5% buffered neutral formalin and embedded in paraffin wax. Sections of 5 μm were cut from each block and stained, primarily with hematoxylin and eosin (H&E), for histopathological study as reported previously.[28,31]

2.8 Determination of serum PR

For the determination of PR concentration, 100 μL of serum sample was denaturized with 10 μL of trichloroacetic acid (10 M) and centrifuged at 4000 rpm for 5 min before analysis. PR concentration was determined using high-performance liquid chromatography with UV-Vis detection coupled with a photodiode array (HPLC-PDA), as described previously with some modifications.[35] Briefly, the mobile phase consisted of a mixture of sodium sulfate (0.01 M, pH 2.5 adjusted with trichloroacetic acid 0.1 M) and acetonitrile (40 : 60, v/v) at a flow rate of 1.0 mL min^{-1}. The PR separation was performed by isocratic elution of the mobile phase through a Sunfire C18 column (150 mm × 4.6 mm, 5.0 μm particle size). The column temperature was maintained at 25 °C, the UV-Vis detection wavelength was set at 243 nm, and the injection volume was 50 μL. The run time for each sample was 5 min and the PR retention time was 4.2 min. The lower limit of quantification (LLOQ) was determined (0.1 μg mL^{-1}). The PR calibration was linear from 0.1 to 100 μg mL^{-1} ($r = 0.999$). Finally, quality control samples at low, medium and high concentrations (0.2 μg mL^{-1}, 20.0 μg mL^{-1} and 50.0 μg mL^{-1}, respectively) were injected to determine the intra- and inter-day precision and accuracy of the LLOQ and the coefficient of variation (CV%) was within the acceptable limit of 10%.

2.9 Biochemical parameters

Serum alanine aminotransaminase (ALT) and aspartate aminotransferase (AST) activities were spectrophotometrically determined using 2,4-dinitrophenylhydrazine at 505 nm according to the kit protocols (Biomaghreb, Tunisia; Randox, United Kingdom) as described previously.[28,31] Creatinine levels were spectrophotometrically determined using commercial diagnostic kits (Biomaghreb, Tunisia; Randox, United Kingdom). Serum levels of TNF-α were measured using a Quantikine ELISA kit (R&D Systems, France). Superoxide-dismutase (SOD) activity and oxidized glutathione/total glutathione (GSSG/TGSH) ratio were determined as previously described,[31,36] where TGSH is the sum of reduced (GSH) and oxidized glutathione (GSSG).

2.10 TiNTs biodistribution

In order to determine the TiNTs biodistribution profile, serum, urine, feces, and organs including stomach, jejunum, ileum, colon, liver, spleen, lungs, heart and kidneys were digested with nitric acid (4 N) for titanium level determination by ICP-OES, as reported previously.[28] The quantification threshold was fixed at 0.1 μg mg^{-1} for tissues and feces and at 0.06 μg μL^{-1} for urine and serum.

2.11 TEM analysis of jejunum and FEG-SEM

For TEM analysis, fragments of rat jejunum were cut into 1 mm^2 cubes and fixed by immersion in 2.5% glutaraldehyde, 2% paraformaldehyde, 2 mM $CaCl_2$, and 0.1% tannic acid previously prepared in 0.1 M cacodylate buffer (pH 7.4), as described previously.[31] Then, ultrathin sections of 90 nm were cut from the dried blocks with a diamond knife on an LBK Ultramicrotome Leica UCT and stained with 0.5% aqueous uranyl acetate followed by Reynold's lead citrate. The observation was performed with a Tecnai G2 at 200 kV (FEI, Netherlands) and images were acquired with a Veleta camera (Olympus, Japan).

Field emission gun scanning electron microscopy (FEG-SEM) of feces (collected from the colon) was carried out using a JEOL JSM 6335F microscope at 15 kV coupled with an Oxford Instruments X-Max 80 mm^2 unit.

Open Access Article. Published on 25 April 2023. Downloaded on 1/10/2026 11:10:29 PM.
This article is licensed under a Creative Commons Attribution-NonCommercial 3.0 Unported Licence.

2.12 Statistics

Results are presented as the mean ± standard deviation of the mean of at least three determinations ($n = 3$). Comparisons with the control were performed using the Tukey HSD test. All analyses were performed using the Statistical Package for the Social Sciences (SPSS) software (version 12 for Windows, SPSS Inc., Chicago, IL, USA). A value of $p < 0.05$ was considered statistically significant.

3. Results

3.1 TiNTs characterization and stability

After hydrothermal synthesis, the physical properties of the TiNTs, including size, shape and crystallinity, were confirmed by SEM, TEM and XRD analysis, as summarized in Fig. 1. The SEM images (Fig. 1A and B) show the surface morphology of TiNTs, corresponding to elongated tunable tubes with lengths ranging between 80 nm and 1 μm. The transmission electron microscopy image (Fig. 1C) shows the typical morphology of hollow multi-walled nanotubes open at both ends with a size of 8–10 nm at the outer diameter and 4 nm at the inner diameter. The distinctive structure and crystallinity of these nanomaterials were confirmed by XRD analysis (Fig. 1D), as described previously.[14,15,28] Additional analyses were performed to characterize TiNTs using TGA, FTIR spectra and N_2 sorption isotherms. TGA measurements of pristine TiNTs (Fig. 2A) show a single stage weight loss of roughly 10% between 120 °C and 200 °C which is ascribed to the release of water molecules physisorbed on the surface and in the pores, as described in our previous works.[15] In the FTIR spectrum (Fig. 2B), two bands at 3400 cm^{-1} and 3040 cm^{-1}, which are characteristic of TiNTs, are easily detected and are attributed to the OH stretching vibration and the alkene aromatic C–H stretching, respectively.[15] Finally, the N_2 sorption capacity of TiNTs indicated a high porosity, with a Brunauer–Emmett–Teller (BET) surface area (S_{BET}) of 270 $m^2\ g^{-1}$.

Regarding the stability, the level of Ti released over 24 h from degraded nanotubes in intestinal medium was around 1% (±0.02), proving high stability. Likewise, for 6 h of gastric incubation, the level of Ti released from degraded nanotubes was below 2%, but it then increases progressively to reach 10.2% (±1.2) at 24 h. This was confirmed by N_2 sorption thermograms, indicating a loss of the TiNTs porosity (≈8.4%) under acidic conditions; indeed, the S_{BET} of the original TiNTs shifts from 270 to 242 $m^2\ g^{-1}$ (Fig. 2C). Taken together, no morphological changes were observed in the crystalline structure compared with those of the pristine TiNTs, as confirmed by the XRD patterns (Fig. 1E), confirming the high stability of TiNTs incubated under GI conditions at 37 °C for 24 h.

3.2 Paracetamol/TiNTs loading and release

The PR/TiNTs loading was carried out using a fixed concentration of PR (2 mg mL^{-1}) incubated with different ratios of TiNTs in a simulated intestinal environment at 37 °C and neutral pH (Ringer's solution, pH = 7.2) to determine the maximum adsorption capacity of the nanomaterials for paracetamol. As

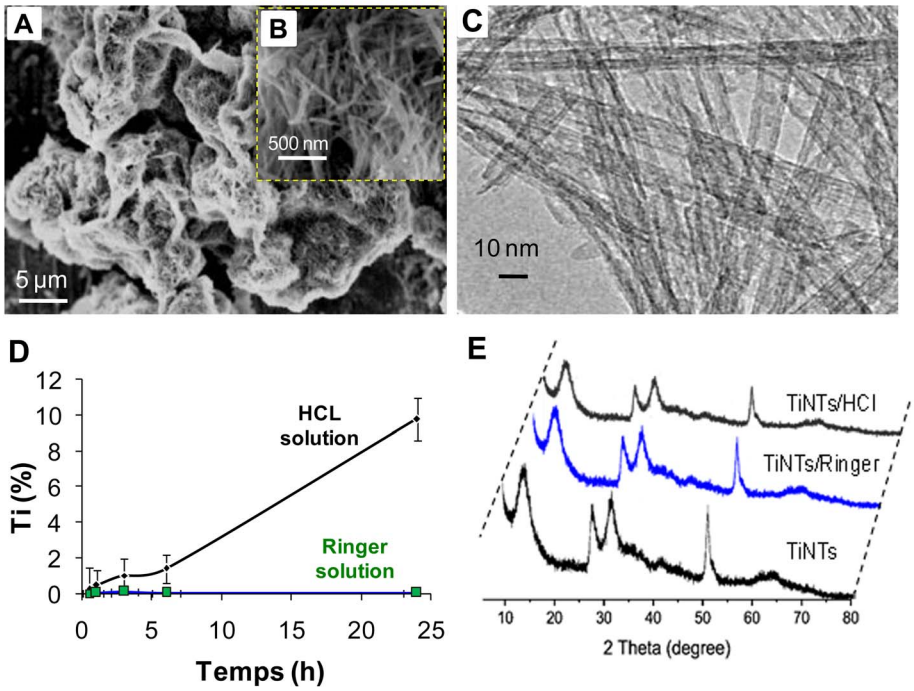

Fig. 1 Characterization of titanate nanotubes (TiNTs). (A and B) SEM images of TiNTs; (B) is a magnification of (A). (C) TEM images of TiNTs showing tubular shape of TiNTs. (D) Degradation of TiNTs under simulated gastric (acidic solution) and intestinal media (Ringer's solution) determined *via* the amount of Ti released after 24 h of stirring at 37 °C. All experiments were carried out in triplicate ($n = 3$). (E) XRD patterns of TiNTs after 24 h of incubation in simulated gastric and intestinal media compared with the XRD pattern of pristine TiNTs.

 © 2023 The Author(s). Published by the Royal Society of Chemistry

Open Access Article. Published on 25 April 2023. Downloaded on 1/10/2026 11:10:29 PM.
This article is licensed under a Creative Commons Attribution-NonCommercial 3.0 Unported Licence.

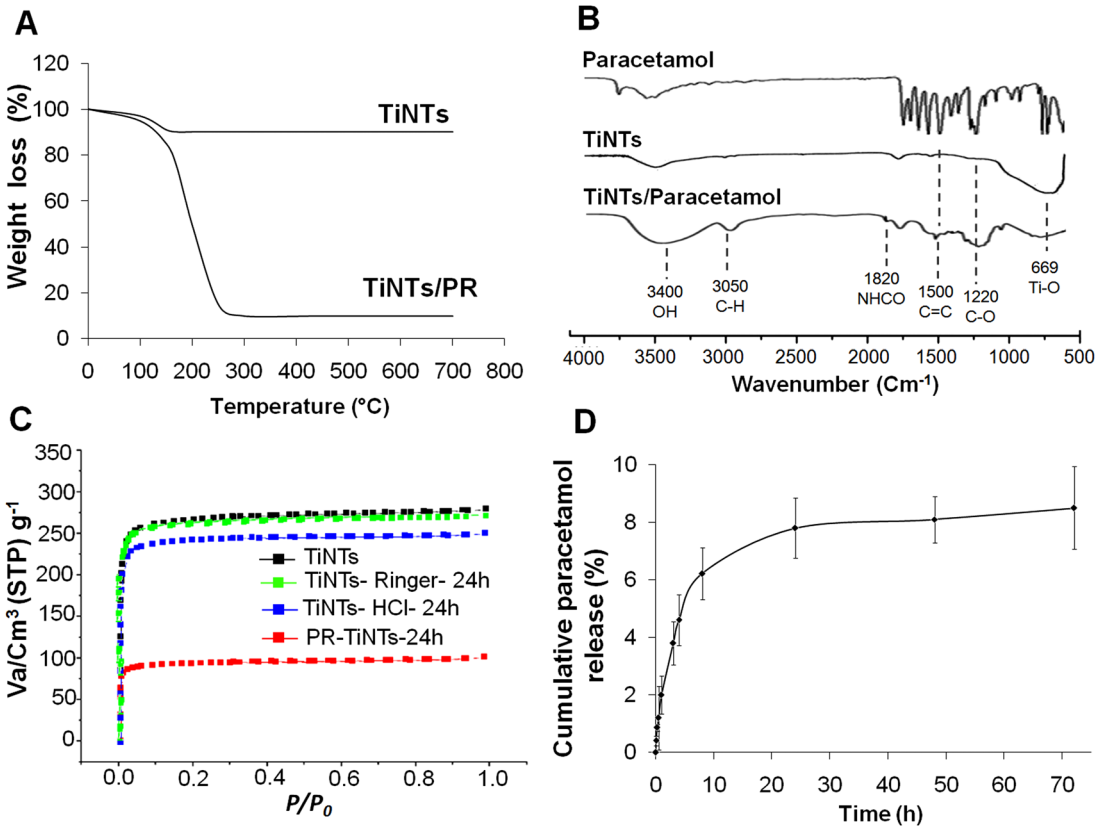

Fig. 2 (A) TGA measurements of empty TiNTs samples and paracetamol (PR)-loaded TiNTs (PR/TiNTs). (B) FTIR spectra of PR, TiNTs and PR/TiNTs. (C) N_2 sorption isotherms at 77 K of pristine TiNTs, PR/TiNTs and TiNTs after 24 h of incubation in Ringer's solution (pH = 6.8) or HCl at 37 °C. PR/TiNTs compared to TiNTs show a decrease in N_2 uptake capacity (≈66%) which is related to the PR loading. (D) Cumulative release of PR in Ringer's solution at 37 °C under continuous stirring up to 72 h. All experiments were carried out in triplicate ($n = 3$).

shown in Table 1, the PR-TiNTs loading increases linearly from 3 h to 6 h to reach a maximum at 24 h of incubation. As the molar ratio increases, the PR loading increases, with the highest values being recorded for the 1 : 4 and 1 : 5 molar ratios.

The loading capacity of TiNTs with the highest molar ratios was compared to those of Norit® activated charcoal (CH) in the same conditions. As shown in Table 2, PR-CH shows lower amounts compared to TiNTs. Indeed, PR-CH loading with molar ratios of 1 : 4 and 1 : 5 increases progressively to reach 15.5–12.62% at 3 h and 35.50–33.62% at 6 h, followed by a decrease to 24.10% and 20.12%, respectively, after 24 h of incubation.

Furthermore, analysis of the FTIR spectrum of PR/TiNTs shows several new peaks compared to the spectra of PR and empty TiNTs, indicating the entrapment of the drug inside the nanomaterials (Fig. 2B). The peaks at 1220 cm^{-1} and 1500 cm^{-1} are related to C–O and C=C, respectively,[15] and the peak at 1820 cm^{-1} is related to NCOH. Likewise, a new band observed at 3050 cm^{-1} is attributed to alkene and aromatic C–H stretching.[15] Finally, a characteristic band at 3400 cm^{-1} present in both the empty TiNTs and PR/TiNTs spectra was related to the OH stretching vibration.[15] In the thermogravimetric analysis of PR/

Table 1 Evolution of paracetamol (PR) removal under simulated intestinal conditions (% of adsorbed paracetamol) using titanate nanotubes (TiNTs)

	PR-TiNTs loading (%)		
Ratios	3 h	6 h	24 h
1 : 0.5	9.80 (±1.04)	20.80 (±3.20)	26.80 (±1.64)
1 : 1	15.40 (±4.08)	28.10 (±4.12)	35.40 (±6.10)
1 : 2	25.20 (±5.20)	40.20 (±7.30)	50.20 (±8.40)
1 : 4	38.32 (±6.02)	52.32 (±9.22)	68.40 (±6.32)
1 : 5	40.22 (±5.30)	58.22 (±6.11)	70.10 (±8.52)

Table 2 Evolution of paracetamol (PR) removal under simulated intestinal conditions (% of adsorbed paracetamol) using Norit® activated charcoal (CH)

	PR-CH loading (%)		
Ratios	3 h	6 h	24 h
1 : 4	15.50 (±1.40)	35.50 (±4.30)	24.10 (±5.30)
1 : 5	12.62 (±1.20)	38.62 (±5.10)	20.12 (±4.20)

Open Access Article. Published on 25 April 2023. Downloaded on 1/10/2026 11:10:29 PM.
This article is licensed under a Creative Commons Attribution-NonCommercial 3.0 Unported Licence.

TiNTs, the thermograms show different weight losses (Fig. 2A); the first is between 50 and 120 °C, corresponding to the loss of water and ethanol, and then a more differentiated second (from 150 to 250 °C) corresponds to PR loss. The amount of PR was estimated using the weight loss of mg of PR per 100 mg of dry TiNTs and was approximately 68 wt%. In addition, the N_2 sorption isotherms (Fig. 2C) indicated that the amount of PR entrapped by TiNTs is about 66%, since the S_{BET} of the empty TiNTs decreases from 270 m^2 g^{-1} to 90 m^2 g^{-1} after PR entrapment. Taken together, we can consider that PR/TiNTs loading is around 70%, consistent with a relatively high drug-TiNTs affinity. Finally, concerning the PR release profile under intestinal conditions (Fig. 2D), results show that PR concentration increases progressively to achieve a cumulative release of less than 10% after 72 h, indicating a sustained release.

3.3 The oral detoxification efficiency of TiNTs *in vivo*

The efficiency of TiNTs as a detoxifying agent in rats overdosed with PR was studied and compared to that of CH. In this regard, serum concentration of PR was determined at 4 h and 24 h post poisoning in all overdosed animals. In the positive control group (PR-24 h), the serum concentration of PR after oral administration of 2 g kg^{-1} was 553.3 (±85.20) μg mL^{-1} at 4 h and declined to 297.2 (±96.1) μg mL^{-1} at 24 h (Fig. 3). In contrast, the administration of CH (1 g kg^{-1}) 1 h after rat poisoning significantly reduced by 40% the absorption of PR compared to the positive control group to achieve 328.2 (±89.10) μg mL^{-1} at 4 h. In contrast, no significant decrease of serum PR concentration was observed in the presence of CH at 24 h post poisoning. In the case of TiNTs (1 g kg^{-1}), the serum concentration of PR decreased by 64.2% at 4 h compared to that of the positive control group to achieve 191.2 (±18.6) μg mL^{-1}. Remarkably, at 24 h post poisoning, TiNTs reduced the amount of PR by 92% to achieve 21.8 (±3.15) μg mL^{-1}, indicating that TiNTs are endowed with a detoxification efficiency significantly higher than that of CH. These results unequivocally confirm the lower absorption of PR and, thus, the efficiency of TiNTs in the detoxification of PR-overdosed rats.

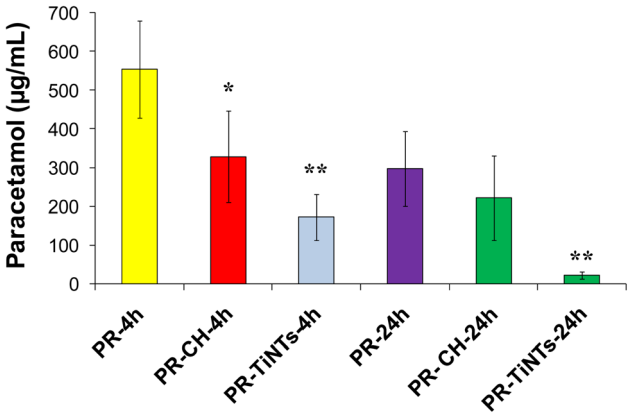

Fig. 3 Serum levels of paracetamol (PR). Results are representative of six independent animals in each group (means ± SD, $n = 6$). Statistical significance was determined by Tukey HSD test (*$p < 0.05$, **$p < 0.01$).

3.4. Animal behavior and histopathological examinations

After 1 h of poisoning, the animals showed a decrease in exploratory behavior (locomotion, sniffing, and standing on hind legs), an arched back and half-closed or squinted eyes. These symptoms indicated animal pain as described for paracetamol intoxication.[37] These symptoms persisted for a period of 24 h in the positive control group of animals treated only with PR (PR-24 h) until their sacrifice, while they disappeared progressively after the oral administration of CH or TiNTs. Histopathological examination of liver, stomach, jejunum, and kidneys showed a significant protective effect of TiNTs against PR poisoning. Microscopic examination of the livers of control rat groups, treated only with Ringer's solution, CH or TiNTs, revealed normal hepatic parenchyma architecture without apparent changes in the hepatocyte structure such as hypertrophy or necrosis (Fig. 4). However, numerous necrotic hepatocytes and abundant neutrophil infiltrate were observed around the central veins of the livers of rats overdosed with PR, suggesting acute inflammation and liver damage due to the accumulation of PR (Fig. 4). The toxic PR effects were reduced in the livers of rats co-treated with CH until 24 h, when rare necrotic hepatocytes surrounded by neutrophils were observed. Concerning the toxic PR effects on the livers of rats co-treated with TiNTs, only rare neutrophils were observed in the hepatic parenchyma around the central vein without hepatocyte necrosis, indicating that TiNTs are more efficient than CH in protecting the liver against PR poisoning.

The stomach histology of the Ringer's-, TiNTs- and CH-treated animals showed normal gastric mucosa consisting of a superficial layer of foveolar cells and a deep layer of gastric glands. In contrast, stomach sections of the PR-overdosed rats show significant histological changes expressed by ulcer formation with cellular desquamation and necrosis of the mucosal epithelium (Fig. S1,† PR-24 h red arrows). In contrast, co-treatment with TiNTs (PR-TiNTs-24 h) revealed a mucosal architecture free from any pathological changes induced by PR, except slight cellular desquamation (red arrow), confirming the gastro-protective effect of TiNTs located on the surface of the mucous cells (black arrow). Note that the TiNTs protection effect is higher than that of CH since the cellular desquamations are more numerous in the stomachs of rats overdosed with PR and co-treated with CH (PR-CH-24 h).

In the intestinal tract, jejunum histology (Fig. 5) showed a significant amount of TiNTs material adhered to the intestinal microvilli, which might prevent intestinal PR absorption. In addition, the presence of totally normal intestinal epithelia with intact mucosa, long and slender microvilli topography covered by both columnar absorptive with brush border and goblet cells and intestinal crypts containing different cell types supports the absence of any severe toxicity in the TiNTs group (TiNTs-24 h *vs.* control group). In contrast, the administration of a PR overdose produced focal erosions in the intestinal mucosa, showing extensive intestinal damage (Fig. 5A, PR-24 h). In particular, we can observe the destruction and shortening of villi and cellular desquamation accompanied by loss of villous relief and altered enterocyte surfaces and brush borders. Remarkably, the PR-

 © 2023 The Author(s). Published by the Royal Society of Chemistry

Open Access Article. Published on 25 April 2023. Downloaded on 1/10/2026 11:10:29 PM.
This article is licensed under a Creative Commons Attribution-NonCommercial 3.0 Unported Licence.

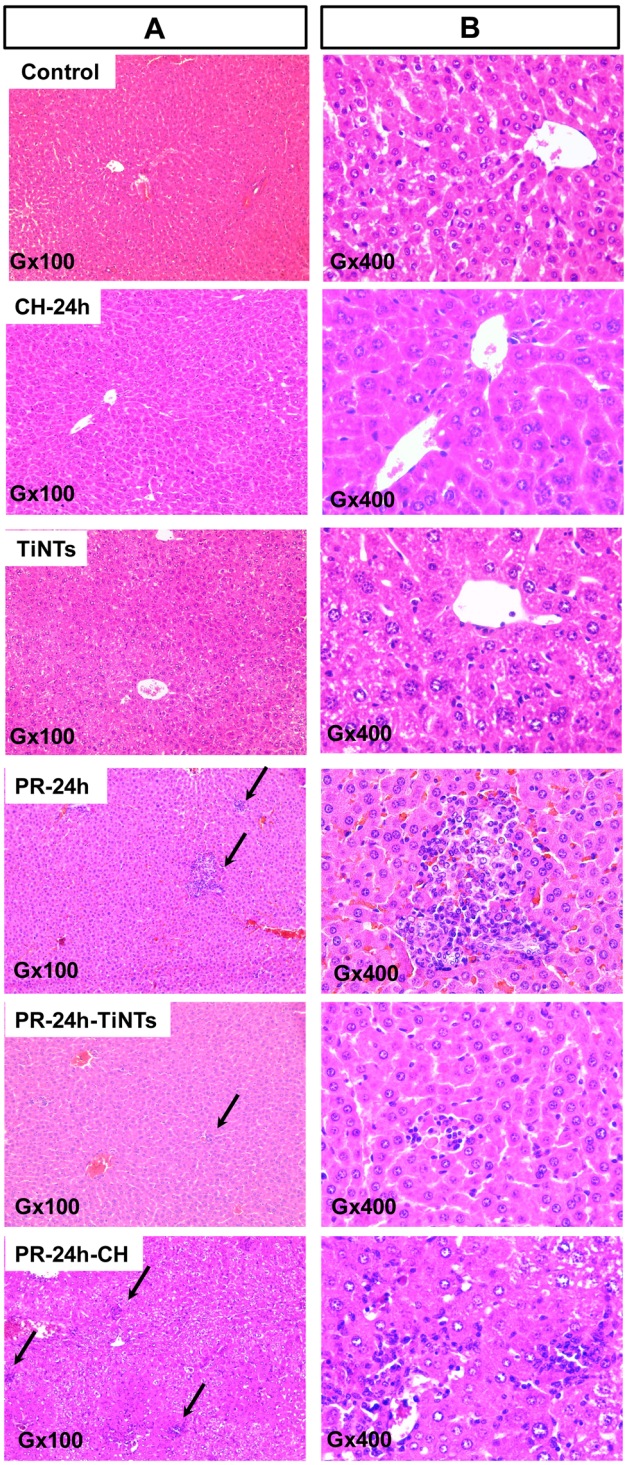

Fig. 4 (A) Histological sections of rat livers 24 h after Ringer's, TiNTs, CH (negative controls), PR (positive control), PR-TiNTs and PR-CH administration. Arrows indicate hepatic neutrophil infiltrations. (B) is a magnification of (A).

TiNTs-24 h group showed reasonably well-preserved jejunum epithelia without any histological lesions, in contrast to the PR-CH-24 h which present cellular desquamation and altered enterocyte surfaces and brush borders. Although the normal villous relief was focally modified due to swelling and fusing of the villi in PR-TiNTs-24 h, no other alteration of the epithelium layer was observed. TiNTs aggregates remain adhered to the intestinal villi, forming a large compact cluster with a size ranging between 500 nm and 2 μm, as shown in the TEM image (Fig. 5C), thus acting as a barrier to prevent the absorption of PR and protecting intestinal mucosa against PR toxicity. Remarkably, the TiNTs possess high *in vivo* stability since they retained their tunable structure all along the GI tract until their excretion by defecation, as visually confirmed by field emission-gun scanning electron microscopy of feces (Fig. S4†). In contrast, activated charcoal crystals were observed to be less condensed across the villi, as revealed by TEM image (Fig. 5C), probably due to their higher-sized particles which decrease their internalization between the intestinal villi.

The histology of the kidneys was also studied as elimination of PR overdose can lead to kidney failure. Microscopic examination of the kidneys of all control groups (orally treated with Ringer's solution, CH or TiNTs at 24 h) showed normal kidney architecture characterized by minimal capsular spaces and classical glomerulus (*G*) structure intimately surrounded by the Bowman's capsule (Fig. S2†). PR poisoning induces enlargement in the Bowman range, with tubule dilatation and hyperemic vessels close to neutrophile infiltration around the glomerulus, which indicates an inflammation process and kidney damage. Co-treatment with TiNTs (Fig. S2,† PR-24 h-TiNTs) reduces this damage; indeed, the glomerulus conserved its classical structure in addition to quite evident dilatation observed in the tubules. In contrast with the TiNTs co-treatment, CH was insufficient to protect the kidneys from inflammation induced by PR, with neutrophile infiltration and hyperemic vessels remaining around the glomerulus (Fig. S2,† CH-24 h-TiNTs).

3.5. Biochemical tests

The activities of the typical biochemical markers of hepatic cytolysis (serum alanine aminotransferase (ALT) and aspartate aminotransferase (AST))[38] and kidney function (serum creatinine) were monitored to determine the effects of PR poisoning and detoxification by TiNTs and CH on organ function. In addition, oxidative stress markers, including blood superoxide dismutase and the oxidized glutathione/total glutathione (GSSG/TGSH) ratio were determined. Finally, LDH and TNF-α markers were determined to analyze tissue damage and inflammation response, respectively. As shown in Fig. S3A and B,† no significant differences in the serum ALT and AST activities were observed in the control groups 24 h after oral treatment with Ringer's solution, TiNTs or CH, as confirmed by the Tukey HSD test (*$p < 0.05$, **$p < 0.01$). Normal ALT activity ranges between 31.25 (±10.62) and 39.60 (±8.30) IU L^{-1}. In contrast, intoxication with PR induces a significant increase of ALT activity up to 170.8 (±33.62), five times higher than that in the control groups. Co-treatment with CH led to a significant attenuation of the increase of this activity. This attenuation was more expressed in the presence of TiNTs in PR-overdosed rats. Indeed, ALT activity declined significantly to 52.25 (±24.85) IU L^{-1} in the PR-TiNTs-24 h group *versus* 105.75 (±18.84) IU L^{-1} in

Open Access Article. Published on 25 April 2023. Downloaded on 1/10/2026 11:10:29 PM.
This article is licensed under a Creative Commons Attribution-NonCommercial 3.0 Unported Licence.

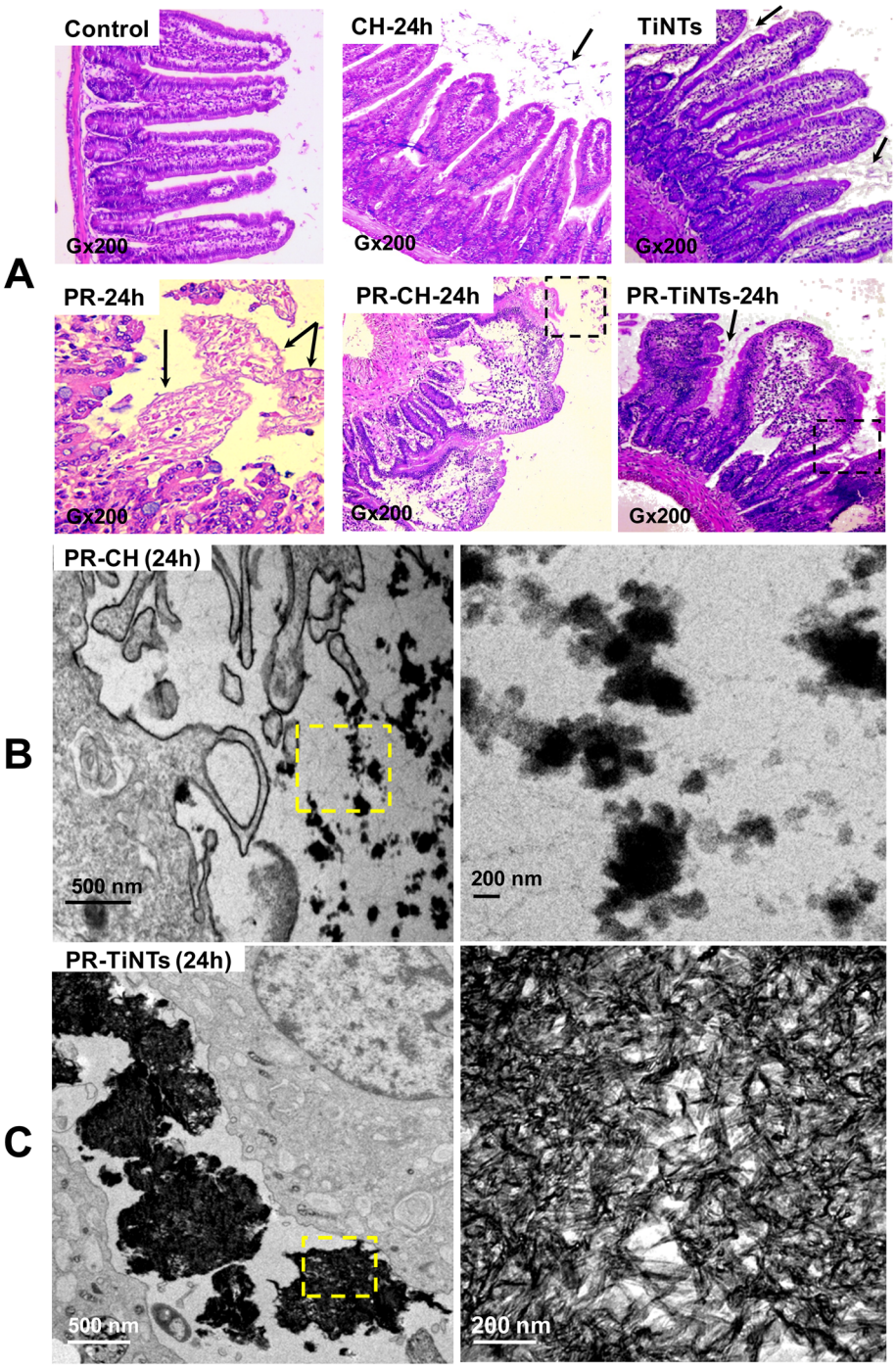

Fig. 5 (A) Histological sections of rat jejunum 24 h after Ringer's, TiNTs, CH (negative controls), PR (positive control), PR-TiNTs and PR-CH administrations. Sections are stained with H&E. (B) TEM images of PR-CH-24 h rat jejunum; the right image is a magnification of the square area selected in the left image, showing aggregation of activated charcoal crystals dispersed across the villi. (C) TEM images of PR-TiNTs-24 h rat jejunum; the right image is a magnification of the square area selected in the left image, showing aggregation of crystal TiNTs adhered across the villi.

the PR-CH-24 h group. Moreover, the serum level of TNF-α marker indicated that poisoning with PR stimulated an acute inflammatory response in overdosed rats. Indeed, the TNF-α level increased approximately four times compared to those of the control groups, reaching 65.2 (±7.8) pg mL^{-1} (Fig. S3D†). In contrast, the level of TNF-α in rats overdosed with PR decreases to 30.5 (±6.2) in the presence of TiNTs *versus* 48.35 (±7.6) pg mL^{-1} in the presence of CH, indicating that TiNTs were more efficient at avoiding acute inflammation than CH. Regarding kidney function and tissue damage, serum creatinine and LDH level variations show that the presence of TiNTs significantly protects organs against acute toxicity caused by PR poisoning

 © 2023 The Author(s). Published by the Royal Society of Chemistry

Open Access Article. Published on 25 April 2023. Downloaded on 1/10/2026 11:10:29 PM.
This article is licensed under a Creative Commons Attribution-NonCommercial 3.0 Unported Licence.

(Fig. S3B and C†). The levels of these markers decrease significantly compared to those of the rats overdosed with PR and become similar to those of the control groups. Finally, the effects of PR poisoning on the endogenous antioxidant system, including blood superoxide dismutase (SOD) and the glutathione system, were studied (Fig. S3E and F†). Erythrocyte SOD's enzymatic activities increase significantly in PR-24 h, PR-TiNTs-24 h and PR-CH-24 h compared to those in the control groups. However, the increases of the GSSG/TGSH ratio in the rats overdosed with PR (PR-24 h) and PR-CH-24 h can reach about 6 to 7 times the GSSG/TGSH ratio of the control groups, reflecting the intensity of the oxidative stress induced by the metabolism of PR. Co-treatment with TiNTs (PR-TiNTs-24 h) significantly prevents the increase of the GSSG/TGSH ratio. Compared to the control groups, the increase of GSSG/TGSH in PR-TiNTs-24 h was only about 3 times.

3.6. Biodistribution of TiNTs

24 hours after the administration of TiNTs in both groups of rats, the rats treated only with nanotubes (TiNTs-24 h group) and those overdosed with PR (PR-TiNTs-24 h), we determined the levels of TiNTs in the different animal matrices *via* the concentration of Ti. The results are summarized in Table 3. We also present the percentage of TiNTs in each matrix (% TiNTs per g of solid matrix or % TiNTs per L of liquid matrix) compared to the administered dose. As shown in Table 1, the biodistribution profile of TiNTs is similar in both rat groups without any statistical differences, as confirmed by the Tukey HSD test (*$p < 0.05$, **$p < 0.01$). This indicated that PR poisoning did not affect the biodistribution of TiNTs, which have a heterogeneous biodistribution profile depending on the biological matrix type. The percentage of TiNTs in the GI tract and feces represent about 80% of the administrated dose (4.4% in stomach, 2.1% in duodenum, 32.6% in jejunum, 8.4% in ileum, 19.01% in colon and 14.04% in feces). Further, only approximately 10% of the orally administrated TiNTs dose was distributed in the blood, liver, spleen, and brain, and thus was eliminated in urine by the kidneys. Note that TiNTs were undetectable in the lungs and heart.

Table 3 Concentration of titanium (μg mg^{-1} of tissue or mL of urine or serum) determined by ICP-OES in organs, serum, urine, and feces 24 h after the oral administration of TiNTs (1 g kg^{-1}). Each value represents a mean from 6 independent experiments ± SD ($n = 6$). For each suspension, 3 measurements were performed. ND = not determined

	Ti (μg mg^{-1} of organ or mL of liquid)			
	Control	TiNTs	PR-TiNTs	TiNTs (%)
Blood	0.1 ± 0.03	1.08 ± 0.13	0.92 ± 0.09	1.84
Stomach	0.12 ± 0.08	1.3 ± 0.12	2.2 ± 0.72	4.40
Duodenum	0.09 ± 0.01	2.09 ± 0.42	1.29 ± 0.51	2.10
Jejunum	0.2 ± 0.01	18.4 ± 3.12	16.3 ± 2.10	32.60
Ileum	0.8 ± 0.03	5.2 ± 1.02	4.2 ± 0.90	8.40
Colon	0.6 ± 0.01	10.4 ± 3.10	9.5 ± 2.30	19.01
Liver	0.2 ± 0.04	0.58 ± 0.12	0.86 ± 0.17	1.72
Spleen	0.52 ± 0.02	0.8 ± 0.33	1.08 ± 0.14	2.16
Kidneys	0.32 ± 0.03	0.15 ± 0.07	0.22 ± 0.08	0.44
Feces	ND	5.82 ± 1.23	7.02 ± 1.60	14.04
Urine	ND	0.8 ± 0.02	0.64 ± 0.07	1.28
Brain	0.2 ± 0.06	1.04 ± 0.40	1.20 ± 0.82	2.40
Lungs	ND	ND	ND	ND
Heart	ND	ND	ND	ND

4. Discussion

In this work, we used TiNTs as a detoxifying agent. The choice of these materials is not only based on its perfect biocompatibility[17] but also on the simplicity of its hydrothermal synthesis and its low-cost compared to MOFs. As reported in our previous work, the hydrothermal synthesis of MIL-127 was carried out with a mixture of iron perchlorate hydrate and 3,3′,5,5′-azobenzenetetracarboxylic acid as the organic linker in dimethylformamide (DMF) and hydrofluoric acid as solvent.[15] The 3,3′,5,5′-azobenzenetetracarboxylic acid is not available commercially and needs to be synthesized separately in the laboratory using 5-nitroisophthalic acid, glucose and sodium hydroxide. Consequently, MIL-127 synthesis is costly and requires time and many steps of purification due to the presence of toxic solvents. Likewise, MIL-125 synthesis requires the incubation of 1,4-benzenedicarboxylic acid as the organic linker and titanium isoproproxide $Ti(OiPr)_4$ in a solution of DMF.[16] However, for TiNTs, the synthesis is simpler, requiring only TiO_2 as precursor and NaOH. The synthetic yield is another advantage for TiNTs. Indeed, we can obtain more than 5 g of TiNTs after one synthesis *versus* 1 g being the largest amount for MOFs.[15–17] Taken together, TiNTs exhibit several features that make it an excellent oral detoxifying agent since it is derived from titanium, which is considered the most biocompatible metal (oral lethal dose $LD_{50} = 25$ g kg^{-1}) and has extremely low absorption when administered orally.[39]

4.1 TiNTs stability and paracetamol loading

Prior to the *in vivo* experiments, both the stability and capacity of PR loading within TiNTs were studied *in vitro*. In contrast to the results in intestinal conditions, the TiNTs were slightly degraded in gastric conditions after 24 h of incubation due to stomach acid, which can dissolve metals at its strongest pH.[40] As shown in our previous work, TiNTs were slowly degraded under lower acidic lysosomal conditions (pH = 2) in Kupffer cells, leading to the generation of short tubular nanotubes and amorphous TiO_2 of irregular sizes.[28] Taking into account that gastric emptying takes 1 to 2 h at most,[36] the TiNTs degradation in this interval of time did not exceed 2%, which confirms the resistance of these nanomaterials to the aggressiveness of the gastric medium. The majority of PR absorption after oral administration occurs in the small intestine[41,42] and very little absorption (≈2%) occurs in the stomach,[43,44] so we studied the TiNTs-PR loading capacity only in intestinal medium. From the loading capacity experiments, we showed that TiNTs were suitable for high PR loading using the largest nanomaterial mass ratios (PR : TiNTs 1 : 4 and 1 : 5). For these mass ratios, the drug loading increases linearly to about 70% in both cases and was maintained after 24 h of incubation, showing a maximum capacity of drug loading within TiNTs, which are able to retain

Open Access Article. Published on 25 April 2023. Downloaded on 1/10/2026 11:10:29 PM.
This article is licensed under a Creative Commons Attribution-NonCommercial 3.0 Unported Licence.

paracetamol in their tunable structure during intestinal transit. Meanwhile, CH-PR loading levels show a progressive increase from 3 h to 6 h of incubation, followed by a decrease at 24 h post incubation, suggesting drug release. Compared with CH, TiNTs show a higher PR loading capacity which increases proportionally with the contact time of the nanomaterials with the drug. Likewise, TiNTs show higher drug loading capacity than MOF materials (70% *versus* 40%).[12] Several works have reported the efficiency of TiNTs as nanocarriers for drug delivery, including for docetaxel,[18] genestein[14] and flumequine,[15] showing high drug loading capacities ranging from 50% to 80% with a perfect sustained release. In contrast with carbon nanotubes[45] or spherical and cubic hybrid MOFs materials,[20,21] it is worth mentioning that the high stability and geometrical properties of TiNTs, including their longer tunable shape and small diameter, play an important role in increasing the drug loading capacity and prolonged release process, as described for genestein and flumequine.[14,15] Interestingly, hydroxyl groups present within both the TiNTs surface and multilayers lead to a stronger ionic interaction between paracetamol and the nanotubes which results in a high drug loading capacity.

4.2 The oral detoxification efficiency of TiNTs *in vivo*

The ability of TiNTs for oral detoxification was evaluated *in vivo* using the PR : TiNTs mass ratio 1 : 5, corresponding to 2 g kg^{-1} of PR and 10 g kg^{-1} of TiNTs, comparable to the dose of CH commonly used in poisoning detoxification.[46] Based on the slower absorption of PR after ingestion of toxic doses, TiNTs or CH were orally administered 1 h after poisoning, which is consistent with the perfect time for detoxification by CH.[47,48] At therapeutic doses, digestive absorption of PR is known to be rapid and almost complete 30 min to 1 h after oral ingestion.[40] However, in overdoses, PR absorption is slower and the plasma peak varies from 1 hour to 4 hours.[40] In these conditions, the ability of CH to adsorb paracetamol, well documented *in vitro*[49] and *in vivo*, ranges between 30 and 45%.[44] Our results were similar: Norit® CH (10 g kg^{-1}), orally administered 1 h after rat overdose poisoning, efficiently and significantly reduced the PR serum concentrations at 4 h post poisoning (40%). There is no consensus on the role of activated charcoal in the treatment of acetaminophen intoxication when administrated 1 h to 2 h post poisoning; it acts to adsorb the drug overdose on its surfaces to render PR unabsorbable by the gastrointestinal tract. However, after this time, CH is inefficient for detoxification, as confirmed at 24 h after intoxication, probably due to drug release in the intestine. In the presence of TiNTs, the reduction of PR absorption was more pronounced than that of CH at 4 h (64%) and 24 h (92%) after poisoning, which suggest that TiNTs can act as a powerful adsorbent. The high drug adsorption effect of TiNTs is clearly attributable to their morphology, longer multilayer nanotubes (80 nm–1 μm) open at both ends, resulting in the high internalization of these nanomaterials across the space separating intestinal villi, thus leading to high drug contact.

Concomitant to the high PR loading ability, PR-loaded TiNTs exhibited good stability during intestinal transit. It can be suggested that PR-retention stability within TiNTs is related to the formation, inside the nanotubes, of crystalline drug grains which become bigger with the increase of drug loading through intermolecular bonding forces, as previously reported for flumequine loading[15] and other drugs.[50] Results from the TEM analysis provide evidence that aggregation of the nanomaterials between the intestinal villi not only hampered the absorption of PR by acting as an absorption barrier, but also made TiNTs aggregates too large to be absorbed by intestinal mucosa, which allows only small particles of up to 10–15 Å to pass through the intestinal barrier.[51] This is consistent with the biodistribution profile of TiNTs showing that about 80% of the administrated dose was distributed in the GI tract and feces *versus* only 10% absorbed and distributed in the bloodstream to reach the liver, spleen, kidneys and brain. Recently, we studied the safety and biodistribution of TiNTs after intravenous administration of 45 mg kg^{-1} in mice.[28] Results confirmed the safety of TiNTs, which were concentrated essentially in the reticuloendothelial system, including the liver and spleen, and then were progressively eliminated from 1 to 45 days through kidney filtration and bile or feces through enterohepatic circulation. This indicated that some of TiNTs disintegrated and detached from the agglomerates, then crossed the intestinal epithelium through transcytosis by M-cell-uptake in Peyer's patches, which constitutes the principle route for digestive absorption reported for TiO_2 nanoparticles.[52] Recent studies reported that oral exposure to nanomaterials mainly concerns the aggregated forms present in food, giving them a micrometric dimension likely to reduce their risk of absorption into the body.[53] However, during the life cycle of a nanomaterial, nanoparticles can detach from an agglomerate or aggregate to be absorbed through the transcytosis process, making it difficult to evaluate their final size.[54] Interestingly, TiNTs aggregates accumulate in the entire GI tract from the stomach to the colon and are defecated in their unchanged tubular shape, as confirmed by field emission-gun scanning electron microscopy observation of feces. Altogether, TiNTs acted as an efficient hepato-protective agent by reducing the absorption of PR, which is known to be hepatotoxic due to the toxicity of its metabolized form *N*-acetyl-*p*-benzoquinone imine (NAPQI).[55–58]

4.3 Biochemical parameters

The most commonly used markers for liver toxicity are liver transaminases (ALT and AST). These enzymes are released into the bloodstream during hepatotoxicity.[59] According to Temple,[60] hepatotoxicity is only considered to exist when the transaminase threshold reaches more than three times the control value. Our results show that intoxication with PR induces a significant increase of liver transaminase activity, reaching 5 times that determined in the control groups. This is expected, since hepatotoxicity is mediated through the metabolism of PR by cytochrome P450, resulting in the formation of the highly toxic NAPQI metabolite in liver. NAPQI causes the depletion of liver glutathione after conjugation to form 3-gluthation-*S*-yl-acetaminophen[27,54] and generates the production of reactive oxygen species (ROS) following its binding to mitochondrial

 © 2023 The Author(s). Published by the Royal Society of Chemistry

Open Access Article. Published on 25 April 2023. Downloaded on 1/10/2026 11:10:29 PM.
This article is licensed under a Creative Commons Attribution-NonCommercial 3.0 Unported Licence.

proteins.[55] The accumulation of ROS stimulates a reaction cascade, the mitogen-activated protein kinase (MAPK) pathway, and leads to the lysis of mitochondria. Further, these cascade reactions lead to hepatocyte necrosis and hepatotoxicity, especially since the mitochondrial antioxidant system is affected.[54,55] To cope with NAPQI-induced oxidative stress, the antioxidant system defense activities increase, including that of SOD, as confirmed in our results.

We also studied the inflammatory response induced by PR intoxication through the TNF-α level, which is marked by a significant increase after the rat overdosing. This cytokine is usually known to activate the recruitment of inflammatory cells and induces oxidative stress.[61,62] Blazka *et al.* reported that TNF-α cytokine levels are increased in PR intoxication.[63] Laskin's study on PR hepatoxicity highlights an activation of Kupffer cells which is accompanied by the modification of immune homeostasis *via* pro- and anti-inflammatory cytokine responses involved in cell proliferation, differentiation and cell death.[64] Regarding the kidney function, the circulating concentration of creatinine was found to increase 24 h after PR intoxication, which is consistent with the results of Bertolini *et al.* showing that NAPQI-induced nephrotoxicity was mediated through the accumulation of NAPQI metabolites and their association with renal proteins.[65] Taken together, the results obtained for transaminases, creatinine, inflammation markers and antioxidant systems (SOD and GSH) after PR intoxication are significantly better with TiNTs treatment than with CH, confirming the detoxifying efficiency of TiNTs and their subsequent histoprotective properties.

5. Conclusion

Owing to their exceptional GI stability, tunable shape and high drug adsorption capacity, TiNTs hold potential as safe and efficient oral detoxifying agents against PR poisoning. TiNTs can achieve higher PR drug loading (≈70%) and a controlled drug release (<10% after 72 h of incubation in simulated intestinal medium). *In vivo* experiments show that TiNTs were more effective than CH in reducing PR absorption and preventing histological damage associated with PR intoxication. TiNTs aggregates accumulate in the entire GI tract from the stomach to the colon without any sign of severe toxicity and are then defecated in their unchanged tubular shape. Biodistribution results are consistent with the low intestinal absorption of TiNTs due the large cluster size of compact aggregate nanomaterials across intestinal villi which form a barrier to PR absorption. In summary, TiNTs have potential for the development of revolutionary detoxifying nanomaterials and provide a long-awaited solution for the treatment of voluntary and accidental intoxications.

Author contributions

The manuscript was written through contributions of all authors. All authors have given approval to the final version of the manuscript.

Conflicts of interest

The authors declare no conflicts of interest.

Acknowledgements

The work was supported by the Tunisian Ministry of Higher Education and Scientific Research (MHESR), grant number LR15INRAP02.

References

1 N. Madge, A. Hewit, K. Hawton, E. J. Wilde, P. Corcoran, S. Fekete, K. V. Heeringen, D. Leo and M. Ystgaard, *J. Clin. Child Psychol.*, 2008, **49**, 667–777.
2 A. G. Kelley, T. Schochet and C. F. Landry, *Ann. N. Y. Acad. Sci.*, 2004, **102**, 27–32.
3 https://wonder.cdc.gov/, accessed 01/05/19.
4 http://www.emcdda.europa.eu/publications/edr/trendsdevelopments/2017, accessed 01/05/19.
5 P. Breen and A. Butt, *Deaths Related to Drug Poisoning in England and Wales: Statistical Bulletin 2021 Registrations*, 2021, https://www.ons.gov.uk/peoplepopulationandcommunity/birthsdeathsandmarriages/deaths/bulletins/deathsrelatedtodrugpoisoninginenglandandwales/2021registrations.
6 M. R. Spencer, A. M. Miniño and M. Warner. *Drug Overdose Deaths in the United States, 2001–2021*, DOI: 10.15620/cdc:122556.
7 P. Le Moigne and M. Morgiève, Les tentatives de suicide par intoxication médicamenteuse volontaire, *Soc. Anthropol.*, 2021, **43**, 83–95.
8 M. Maignan, P. Pommier and S. Clot, *Basic Clin. Pharmacol. Toxicol.*, 2014, **114**, 281–287.
9 G. K. Isbister, F. Downes, D. Sibbritt, A. H. Dawson and I. M. Whyte, *Crit. Care Med.*, 2004, **32**, 88–93.
10 L. M. Graham, T. M. Nguyen and S. B. Lee, *Nanomedicine*, 2011, **6**, 921–928.
11 H. Bae and K. Lee, *Emerg Med J.*, 2007, **24**, 233.
12 S. M. Selbst, *Pediatric Emergency Medicine Secrets*, Saunders Elseiver Inc, Philadelphia, 2015.
13 L. Roivas and P. J. J. Neuvonen, *Pharm. Sci.*, 1992, **81**, 917–919.
14 P. J. Neuvonen and K. T. Olkkola, *Med Toxicol Adverse Drug Exp.*, 1988, **3**, 33–58.
15 S. Rojas, T. Baati, L. Njim, L. Manchego, F. Neffati, N. Abdeljelil, S. Saguem, C. Serre, M. F. Najjar, A. Zakhama and P. Horcajada, *J. Am. Chem. Soc.*, 2018, **140**, 9581–9586.
16 S. Rojas, N. Guillou and P. Horcajada, *ACS Appl. Mater. Interfaces*, 2019, **11**, 22188–22193.
17 T. Baati, B. Kefi, A. Aouane, L. Njim, F. Chaspoul, V. Heresanu, A. Kerkeni, F. Neffati and M. Hammami, *RSC Adv.*, 2016, **6**, 101688.
18 T. Baati, M. B. Brahim, A. Salek, M. Selmi, L. Njim, P. Umek, A. Aouane, M. Hammami and K. Hosni, *RSC Adv.*, 2022, **12**, 5953–5963.

Open Access Article. Published on 25 April 2023. Downloaded on 1/10/2026 11:10:29 PM.
This article is licensed under a Creative Commons Attribution-NonCommercial 3.0 Unported Licence.

19 K. N. Calıs, C. Bayram, E. Erdal, Z. Karahaliloğlu and E. B. Denkbaş, *Mater. Sci. Eng., C*, 2014, **35**, 100–105.
20 C. Moseke, J. M. Bae, S. Jin and S. Oh, *Appl. Surf. Sci.*, 2012, **258**, 5399–5404.
21 A. L. Papa, L. Dumont, D. Vandroux and N. Millot, *Nanotoxicology*, 2013, **7**, 1131–1142.
22 T. Baati, L. Njim, S. Jaafoura, A. Aouane, F. Neffati, N. Ben Fradj, A. Kerkeni, M. Hammami and K. Hosni, *ACS Omega*, 2021, **6**, 21872–21883.
23 S. B. Tiwari and M. M. Amiji, *Curr. Drug Delivery*, 2006, **3**, 219–232.
24 G. F. Paciotti, L. Meyer and D. Weinreich, *Drug Delivery*, 2004, **11**, 169–183.
25 D. Cunha, M. Ben Yahia, S. Hall, S. Miller, H. Chevreau, E. Elkaïm, G. Maurin, P. Horcajada and C. Serre, *Chem. Mater.*, 2013, **25**, 2767–2776.
26 D. H. Mobarak, S. Salah and S. A. Elkheshen, *Pharm. Dev. Technol.*, 2014, **19**, 891–900.
27 M. Salouti and A. Ahangari. *Nanoparticle Based Drug Delivery Systems for Treatment of Infectious Diseases*, InTech, New York, 2014.
28 N. Nistor, C. Jitareanu, O. E. Frasinariu, I. M. Ciomaga, A. L. Rugina and V. Streanga, *Medicine*, 2017, **96**, e5831.
29 F. Rouyer. *Prise en charge des intoxications au paracétamol dans la structure d'urgences du Centre Hospitalier Universitaire nord de la Réunion : étude descriptive*. Doctorat Médecine Générale, France, 2014.
30 L. P. James, L. Letzig, P. M. Simpson, E. Caparelli, D. W. Roberts, J. A. Hinston, T. J. Dayern and W. M. Lee, *Drug Metab. Dispos.*, 2009, **37**, 1779–1784.
31 C. J. Henderson, C. R. Wolf, N. Kitteringham, H. Powell, D. Otto and B. K. Park, *Proc. Natl. Acad. Sci. U. S. A.*, 2000, **23**, 12741–12745.
32 D. H. Smyth, *Biomembranes*, Springer 1st edn, U.K, 1974.
33 A. L. Dickinson, C. Leach and P. A. Flecknell, *Lab. Anim.*, 2009, **43**, 357–361.
34 T. Baati, A. Al-Kattan, M. A. Esteve, L. Njim, Y. Ryabchikov, F. Chaspoul, M. Hammami, M. Sentis, A. V. Kabashin and D. Braguer, *Sci. Rep.*, 2016, **6**, 25400.
35 L. S. Jensen, J. Valentine, R. W. Milne and A. M. Evans, *J. Pharm. Biomed. Anal.*, 2004, **34**, 585–593.
36 T. Baati, F. Bourasset, N. Gharbi, L. Njim, M. Abderabba, H. Szwarc and F. Moussa, *Biomaterials*, 2012, **33**, 4936–4946.
37 A. E. Rupley and D. J. Heard. *Rodent Analgesia, Veterinary Clinics of North America: Exotic Animal Practice*, Elsevier, 2001.
38 B. Halliwell and J. M. C. Gutteridge, *Free Radical Biol. Med.*, 1995, **18**, 125e6.
39 W. S. Cho, B. C. Kang, J. K. Lee, J. Jeong, J. H. Che and S. H. Seok, *Part. Fibre Toxicol.*, 2013, **10**, 9.
40 T. C. Martinsen and R. Fossmark, *Int. J. Mol. Sci.*, 2019, **23**, 6031.
41 S. S. Davis, *Drug Discovery Today*, 2005, **10**, 249–257.
42 T. Ueno, A. Tanaka, Y. Hamanaka and T. Suzuki, *Br. J. Clin. Pharmacol.*, 1995, **39**, 330–332.
43 J. A. Forrest, J. A. Clements and F. F. Prescott, *Clin. Pharmacokinet.*, 1982, **7**, 93–107.
44 M. Sanaka, Y. Koike, T. Yamamoto, S. Mineshita, S. Yamaoka, S. Hirama, H. Tanaka, Y. Kuyama and M. Yamanaka, *Int. J. Clin. Pharmacol. Ther.*, 1997, **35**, 509–513.
45 S. B. Tiwari and M. M. Amiji, *Curr. Drug Delivery*, 2006, **3**, 219–232.
46 O. Lapatto-Reiniluoto, K. T. Kivistö and P. J. Neuvonen, *Br. J. Clin. Pharmacol.*, 1999, **2**, 148–153.
47 C. Bismuth.*Toxicologie Clinique*,Médecine Sciences Flammarion 5èmeed, Paris, 1998.
48 S. E. Farrell, Toxicity, acetaminophen: differential diagnosis and workup, *E-medicine*, 2011, **14**, 102–111.
49 L. C. G. Hoegberg, H. R. Angelo, A. B. Christophersen and H. R. Christensen, *Clin. Toxicol.*, 2002, **40**, 59–67.
50 K. Gulati, K. Kant, D. Findlay and D. Losic, *J. Mater. Chem. B*, 2015, **3**, 2553–2559.
51 T. Suzuki, *Cell. Mol. Life Sci.*, 2013, **4**, 631–659.
52 A. Elder, S. Vidyasagar and L. DeLouise, *Wiley Interdiscip. Rev.: Nanomed. Nanobiotechnol.*, 2009, **1**, 434–450.
53 A. Weir, P. Westerhoff, L. Fabricius, K. Hristovski and N. V. Goetz, *Environ. Sci. Technol.*, 2012, **46**, 2242–2250.
54 Y. Wang, Z. Chen, T. Ba, J. Pu, T. Chen, S. Yanshuang, Y. Gu, Q. Qian, Y. Xu, K. Xiang, H. Wang and G. Jia, *Small*, 2013, **9**, 1742–1752.
55 D. C. Dahlin, G. T. Miwa, A. Y. Lu and S. D. Nelson, *Proc. Natl. Acad. Sci. U. S. A.*, 1984, **5**, 1327–1331.
56 H. Dong, R. L. Haining, K. E. Thummel, A. E. Rettie and S. D. Nelson, Drug Metab, *Dispos*, 2000, **12**, 1397–1400.
57 M. R. McGill and H. Jaeschke, *Pharm. Res.*, 2013, **30**, 2174–2187.
58 M. R. McGill, M. Lebofsky, K. N. Hye-Ryun, M. H. Slawson, M. L. Bajit, Y. Xie, C. D. Williams, D. G. Wilkins, D. E. Rollins and H. Jaeschke, *Toxicol. Appl. Pharmacol.*, 2013, **269**, 240–249.
59 E. G. Giannini, *Can. Med. Assoc. J.*, 2005, **172**, 367–379.
60 R. Temple, *Pharmacoepidemiol. Drug Saf.*, 2006, **15**, 241–243.
61 C. Ju, T. P. Reilly, M. Bourdi, M. F. Radonovich, J. N. Brady, J. W. George and L. R. Pohl, *Chem. Res. Toxicol.*, 2002, **12**, 1504–1513.
62 M. E. Blazka, M. R. Elwell, S. D. Holladay, R. E. Wilson and M. I. Luster, *Toxicol. Pathol.*, 1996, **2**, 181–189.
63 M. E. Blazka, J. L. Wilmer, S. D. Holladay, R. E. Wilson and M. I. Luster, *Toxicol. Appl. Pharmacol.*, 1995, **1**, 43–52.
64 D. L. Laskin and A. M. Pilaro, *Toxicol. Appl. Pharmacol.*, 1986, **2**, 204–215.
65 A. Bertolini, A. Ferrari, A. Ottani, S. Guerzoni, R. Tacchi and S. Leone, *CNS Drug Rev.*, 2006, **12**, 250–275.

 © 2023 The Author(s). Published by the Royal Society of Chemistry